

Ionospheric Response to the May 11, 2024, Geomagnetic Superstorm over Ecuador

Ericson Lopez^{1,2}, Hugo Barbier¹, William Carvajal², Leonel Guamán²

¹Escuela Politécnica Nacional, Facultad de Ciencias, Departamento de Física, Quito, Ecuador

²Escuela Politécnica Nacional, Observatorio Astronómico de Quito/ Observatorio Nacional, Quito,
Ecuador

Key Points:

- Impact of the geomagnetic storm: A G5 geomagnetic storm (10-13 May 2024) caused an unusual drop in Total Electron Content (TEC) above Galápagos, Ecuador.
- Unusual TEC behavior: The drop in TEC during the storm peak was likely due to rapid atmospheric changes, followed by a gradual increase in TEC after the storm.
- Importance of Continuous Monitoring: The study highlights the need for continuous monitoring to understand the effects of geomagnetic storms on satellite communications and navigation systems.

arXiv:2502.04503v1 [physics.space-ph] 6 Feb 2025

Abstract

This study investigates the impact of the G5 geomagnetic storm on Total Electron Content (TEC) derived from the Global Positioning System (GPS) in Galápagos, Ecuador (geographic latitude 0.1807° S, longitude 78.4678° W) during May 10-13, 2024. Using vertical TEC (VTEC) data from a single pseudorandom noise (PRN) code, along with the average VTEC from the same PRN collected over the ten days before the storm, referred to as background TEC, to analyze the variations in TEC.

Our findings indicate that during the main phase of the storm on May 10-11, 2024, TEC experienced a notable decrease, which contrasts with the typical responses observed in previous storms. This decrease can be attributed to rapid recombination processes and potential plasma instabilities triggered by the storm. In the recovery phase following the main storm, a gradual increase in TEC was observed, illustrating the complex dynamics of the ionosphere in response to geomagnetic disturbances.

This study underscores the variability in TEC responses during geomagnetic storms. It highlights the importance of real-time monitoring to improve our understanding of the implications for satellite communication and navigation systems.

Plain Language Summary

In this study, we examined how a strong geomagnetic storm (G5 level) affected the Total Electron Content (TEC) in the atmosphere above Galápagos, Ecuador, from 10 to 13 May 2024. TEC measures the number of electrons in a certain area of the ionosphere that can affect satellite signals. We used data from the Global Positioning System (GPS) to analyze changes in TEC.

Our results showed that during the peak of the storm on 10-11 May 2024, the TEC dropped significantly, which is different from what we usually see in other storms. This drop was likely caused by fast changes in the atmosphere and possible instabilities caused by the storm. After the storm, the TEC gradually increased, showing how the ionosphere can change in complex ways during and after a geomagnetic disturbance.

This study highlights that TEC can respond in different ways during geomagnetic storms and emphasizes the need for continuous monitoring to better understand how these storms affect satellite communications and navigation systems.

1 Introduction

From 10-13 May 2024, an exceptionally strong geomagnetic storm, classified as G5, occurred at the peak of solar cycle 25. This event was significant due to its impact, which resulted from multiple observed coronal mass ejections (CMEs) originating from the Sun (Kwak et al., 2024).

Coronal mass ejections (CMEs) are massive expulsions of plasma and magnetic fields from the Sun's corona into space, capable of significantly influencing Earth's space weather (Shen et al., 2022). These events can cause geomagnetic storms that affect telecommunications, navigation systems, and power grids (Pulkkinen et al., 2017).

Geomagnetic storms arise from the interaction of the solar wind with the magnetic field of the Earth (Sun et al., 2024). These storms can cause large-scale disturbances in the ionosphere, including irregularities and rapid fluctuations in electron content. The resulting variations in vertical total electron content (VTEC) can pose challenges to accurate modeling and prediction (Chen et al., 2024).

Recently, GPS measurements have been utilized to study the effects of geomagnetic storms on total electron content (TEC). Research focused on regions affected by the Equatorial Ionization Anomaly (EIA) is particularly important, as the equatorial plasma fountain is highly sensitive to electrical disturbances (Shagimuratov et al., 2024).

The EIA is mainly associated with the distribution of electron density in the ionosphere rather than directly with the magnetic field of the Earth (Abdu, 2005). However, its presence and behavior are closely linked to the magnetic field, especially its horizontal component at the magnetic equator. The near-horizontal magnetic field lines at the equator are crucial for the formation of the EIA through the equatorial fountain effect (Balan et al., 2018). During the day, solar heating generates an eastward electric field at the equator. This electric field interacts with the Earth's magnetic field to produce an upward drift ($E \times B$). Ionized particles are lifted to higher altitudes by this drift and subsequently move along the magnetic field lines to higher latitudes, creating two crests of high electron density. Enhanced electric fields during storms can intensify this $E \times B$ drift, leading to a more pronounced EIA (Aa et al., 2024).

Geomagnetic storms induce fluctuations in Earth's magnetic field, particularly at high latitudes (Kamide et al., 1998). These fluctuations can propagate to lower latitudes, including the equatorial region. Magnetic field disturbances can induce electric fields and currents in the ionosphere, known as disturbance dynamo effects, which can modify existing ionospheric electric fields (Tahir et al., 2024). During the initial phase of a geomagnetic storm, high-latitude electric fields can penetrate to equatorial latitudes almost instantaneously. These prompt penetration electric fields can enhance the eastward electric field at the equator, increasing the upward $E \times B$ drift and intensifying the EIA.

Geomagnetic storms also cause variations in the Earth's magnetic field, known as magnetic field perturbations, which are recorded as changes in both horizontal and vertical components (Hayakawa et al., 2021). These variations can be observed globally, with more pronounced effects at high and equatorial latitudes as a result of intensified auroral and equatorial currents.

The Equatorial Electrojet (EEJ) typically increases during the daytime; enhanced eastward electric fields boost the EEJ, resulting in a higher magnetic field at ground level in the equatorial region (Yamazaki & Maute, 2017). Conversely, if the electric fields weaken or reverse (for example, during nighttime or due to disturbance dynamo effects), the EEJ diminishes, leading to a decrease in the magnetic field. Enhanced electric fields and intensified ionospheric currents, such as auroral and equatorial electrojets, generally lead to an increase in the magnetic field, particularly noticeable during the main phase of a geomagnetic storm at high and equatorial latitudes. Opposing electric fields, disturbances in ionospheric currents, and the recovery phase of geomagnetic storms can result in a decrease in the magnetic field (Li et al., 2024).

Factors such as geomagnetic storms, solar flares, and other space weather events can induce sudden and severe disturbances in the ionosphere, complicating the generation of accurate VTEC maps during these periods (Chen et al., 2024).

Space weather, primarily driven by solar activity, significantly affects the accuracy of VTEC (Vertical Total Electron Content) maps by introducing variations and disturbances in the Earth's ionosphere (Luo et al., 2023). Key ways in which space weather impacts the accuracy of VTEC maps include increased ionospheric variability and disruptions caused by solar phenomena.

The Dst and Kp indexes are important tools for monitoring and understanding geomagnetic activity (Matzka et al., 2021). These indices track the strength of magnetic storms triggered by solar activity, such as solar flares and CMEs, which can affect the Earth's magnetosphere and ionosphere. The Dst index measures the globally averaged strength of geomagnetic disturbances, quantifying how much Earth's magnetic field is

disturbed during these events (Lin, 2021). It typically ranges from negative values (indicating geomagnetic storm conditions) to positive values (indicating quieter conditions), usually falling between -20 and +20 nanotesla (nT). The Dst index is primarily used to assess the severity and duration of geomagnetic storms, which can impact technological systems such as satellites, power grids, and radio communications. The Kp index measures the level of geomagnetic activity on a global scale, providing a real-time assessment of storm intensity (Matzka et al., 2021). It ranges from 0 to 9, with increasing values indicating higher levels of geomagnetic activity. The Kp index is vital for space weather forecasting, helping predict the impacts of geomagnetic storms on Earth's magnetosphere and technological systems. Both indices are crucial for monitoring and predicting space weather, as they provide quantitative measures of geomagnetic disturbances.

In this study, we examined the effects of geomagnetic storms on GPS-derived VTEC at the Galapagos receiver GLPS (geomagnetic latitude $0^{\circ}44'34.97''S$, geomagnetic longitude $90^{\circ}18'13.2''W$), situated below the crest region of the Equatorial Ionization Anomaly (EIA). Our analysis aimed to correlate the filtered CME data with the geomagnetic indices Dst and Kp, focusing on the impact of the severe geomagnetic storm on 11 May 2024, on variations in GPS-derived total electron content (TEC) in Galápagos, Ecuador. Our results indicated that during the G5 geomagnetic storm of May 2024, vertical TEC (VTEC) values decreased during the main phase of the storm.

2 Procedure to Obtain TEC from GPS Receivers

The ionosphere exhibits a refractive index at radio frequencies that deviates from unity, affecting GPS signals as they travel from the satellite to the ground receiver (Misra & Enge, 2006). A major consequence of this interaction is the additional delay that GPS signals experience while traversing the ionosphere, which is directly proportional to the total electron content (TEC). TEC is defined as the total number of free electrons in a column with a cross-sectional area of 1 m^2 along the path from the satellite to the receiver (Leitinger et al., 2008). GPS data offer a highly effective means of estimating TEC values with improved spatial and temporal coverage (Ciraolo et al., 2007). Given that the frequencies utilized in the GPS system are sufficiently high, the signals are only minimally influenced by ionospheric absorption and the Earth's magnetic field, both in the short-term and during long-term variations in the ionospheric structure (Nagarajoo & Fah, 2013). Each Global Positioning System (GPS) satellite transmits signals at two distinct frequencies: $f_1 = 1575.42\text{ MHz}$ and $f_2 = 1227.60\text{ MHz}$. These signals use two different codes, P1 and P2, as well as two distinct carrier phases, L1 and L2, all derived from a common oscillator operating at 10.23 MHz (GPS.gov, 2001).

In this study, the total electron content slant (STEC) derived from GPS data collected at our zero geographical latitude station in Galápagos islands is converted into the total vertical electron content (VTEC) as described in the literature (Hernández-Pajares et al., 2002):

$$STEC = \frac{1}{40.3} \left(\frac{f_1^2 \cdot f_2^2}{f_2^2 - f_1^2} \right) [(P_1 - P_2) + (\Delta b^s - \Delta b_r)], \quad (1)$$

where b_R and b_S represent the biases of the receiver and satellite, respectively.

The vertical TEC is related to the slant TEC by:

$$VTEC = S(E_l) \cdot TEC, \quad (2)$$

where $S(E_l)$ is the translation coefficient, also known as the mapping function at the ionospheric pierce point (IPP), and it is defined accordingly (B. S. Arora, J. Morgan et al., 2015 & references therein) as:

$$VTEC = \left(\sqrt{1 - \left(\frac{R_T}{R_T + H} \cos(E_l) \right)^2} \right) \cdot STEC \quad (3)$$

E_l indicates the satellite's elevation angle in degrees. VTEC reflects the vertical TEC at the IPP. R_T denotes the Earth's radius (6371 km) and for this study, we have selected an atmospheric height H of 400 km.

The data for this analysis were obtained from GNSS stations in the CDDIS - NASA archive, focusing specifically on the total electron content (TEC) of the GLPS station during the period from May 1 to May 15, 2024. The RINEX data were filtered to include only satellites with an elevation angle above 40 degrees, ensuring a good signal-to-noise ratio. This data was supplemented with records from the magnetic data acquisition system (MAGDAS) sensor at the Quito Astronomical Observatory. Furthermore, the Kp and Dst indices, provided by the GFZ Helmholtz Center, were incorporated for the same date range (GFZ Helmholtz Center, 2024).

Data from the MAGDAS station and TEC were processed using Fourier transform techniques and filtered to eliminate high-frequency noise. Data were organized into averaged blocks to align with the lengths of the Dst and Kp index data, facilitating correlation analysis (Press et al., 1992). Data were initially cleaned by removing outliers using the interquartile range (IQR) method, ensuring data accuracy. Subsequently, the data were grouped by time intervals and stations to calculate descriptive statistics like mean and standard deviation. To enhance the visualization and analysis of trends, spline interpolation was applied to smooth the curves. Using a fast Fourier transform (FFT), the VTEC signal was decomposed into its constituent frequency components, revealing periodic patterns or cyclic variations. To enhance the visualization of long-term trends and eliminate high-frequency noise, a high-pass filter with a cutoff frequency of 0.00001 days was applied. This filtering effectively isolated the lower-frequency components, which are crucial for understanding the physical processes that govern the ionosphere, providing a more refined description of the underlying TEC trends.

3 G5 geomagnetic storm affectation on TEC

We selected the extremely intense geomagnetic storm observed on 11 May 2024 for our study because of its exceptional strength, characterized by a minimum Dst-index of -410 nT and a Kp index of 9. Investigating the ionosphere's response to geomagnetic storms, particularly its impact on Total Electron Content (TEC), is a crucial aspect of space weather research. Normally, the ionosphere exhibits stable and predictable TEC levels, shaped by solar radiation, atmospheric dynamics, and seasonal factors. Under these typical conditions, ionization is predominantly driven by solar ultraviolet (UV) radiation, with electron densities peaking around local noon (Ratovsky et al., 2020).

The intense storm of 11 May 2024 presents a valuable case for examining these processes in greater detail. By tracking the temporal evolution of TEC before, during, and after the storm, we aim to deepen our understanding of the ionosphere's behavior in response to such extreme geomagnetic disturbances. This research can contribute to improving predictive models of space weather impacts, which are crucial to mitigate the effects on satellite communications and navigation systems (Chaitra & Nagaraja, 2024).

During the main phase of a geomagnetic storm, negative storm effects often lead to substantial reductions in electron density, especially at low and equatorial latitudes. The reduced electron density weakens the ionospheric conductivity, thus diminishing current systems such as the equatorial electrojet (EEJ), which, in turn, leads to a reduction in the horizontal magnetic field (Simi et al., 2013). The observed decrease of approximately 30 TEC units during the main phase of the storm can be attributed to a

combination of factors, including enhanced recombination, plasma instabilities, atmospheric dynamics, and the disruption of normal ionospheric processes, all of which contribute to significant electron depletion (Fuller-Rowell et al., 2008)

4 Results and discussion

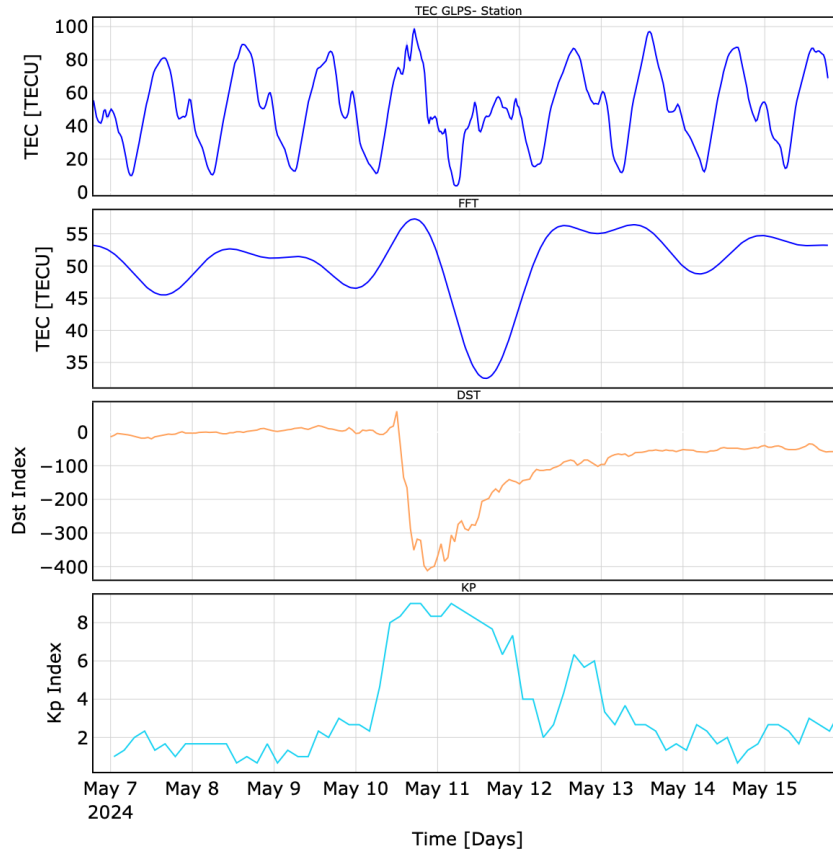


Figure 1. Variation of Total Electron Content (TEC), Dst and Kp indexes, during the main phase of the may 2024, G5 storm

The analysis reveals a strong correlation between the CME (Coronal Mass Ejection) data and both the Dst and Kp indices, as illustrated in the accompanying graphs. This correlation suggests that the CME had a substantial impact on terrestrial geomagnetic indices, consistent with previous studies highlighting the significant influence of CMEs on space weather (Pulkkinen et al., 2017). The global geomagnetic activity on 11 May 2024 reached a Kp index of 9, demonstrating the severity of the geomagnetic storm triggered by a massive CME and energetic solar wind. This event was classified as a G5 (extreme) storm, according to NOAA’s space weather scales.

The Earth’s magnetic field disturbance, quantified by the Kp index, started increasing days before the CME’s impact. The index rose from its normal level of Kp 2 on May 9, 2024, to a peak 9 on May 11, maintaining moderate activity until it returned to baseline on May 15.

The Disturbance Storm-Time (Dst) index, a measure of geomagnetic activity indicating global magnetic field perturbations, reached -410 nT on May 11, 2024. A Dst

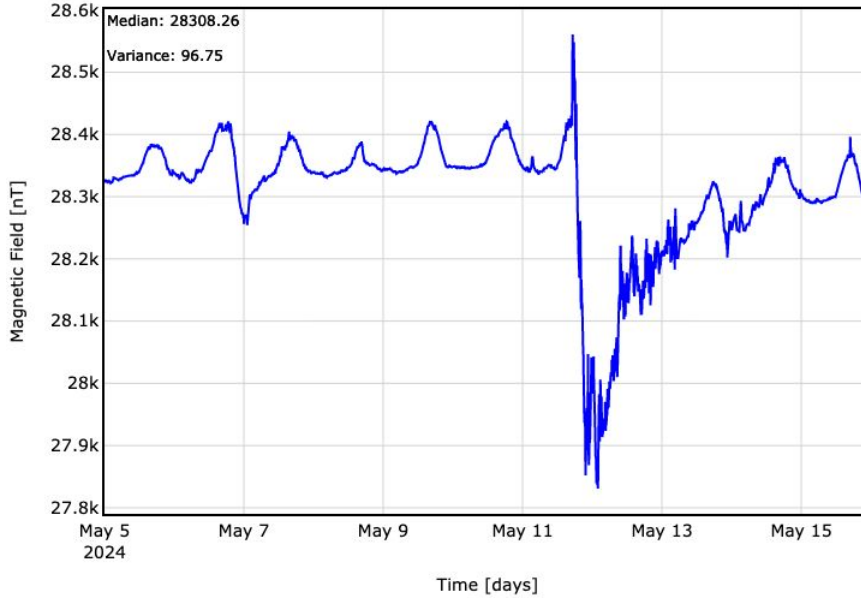


Figure 2. May, 2024 G5 storm, horizontal magnetic field component

value this low signifies an exceptionally severe geomagnetic storm, known to weaken Earth’s magnetic field due to intense solar activity, such as flares or CMEs (Kamide et al., 1998). Geomagnetic storms of this magnitude pose serious risks to satellite operations, potentially disrupting or damaging satellite systems and communications. Moreover, intense geomagnetic storms can induce geomagnetically induced currents (GICs) in power grids, potentially damaging transformers and causing power outages (Pirjola, 2002). While widespread outages were not reported during this storm, localized disruptions and voltage fluctuations occurred, particularly in areas vulnerable to GICs.

High-frequency (HF) radio communications, especially those used in aviation and maritime operations, experienced significant disruption during the storm, particularly in polar regions where geomagnetic disturbances were most severe (Lanzerotti et al., 2001). The storm also produced a remarkable display of auroras, visible in regions far from the poles, including areas where such phenomena are rare. These auroras, observed globally, highlighted the extent of the solar wind’s interaction with Earth’s magnetosphere during this extreme event.

The geomagnetic storm persisted from May 10 to May 15, 2024, with the magnetosphere gradually returning to normal conditions. Reports from the ANEMOS/NKUA team indicate that this G5 extreme storm was caused by multiple CMEs that impacted Earth’s magnetic field between May 10 and 13, intensifying the storm’s duration and severity.

One notable effect of this storm was a significant decrease in the Total Electron Content (TEC), with a drop of nearly 30 units observed in the equatorial region. This reduction, contrary to the expected increase during such events, can be attributed to the unique ionospheric dynamics at low latitudes. In the equatorial ionosphere, processes like the equatorial anomaly and the electrojet are particularly sensitive to geomagnetic disturbances, leading to complex responses (Fuller-Rowell et al., 2008). Disruptions to the

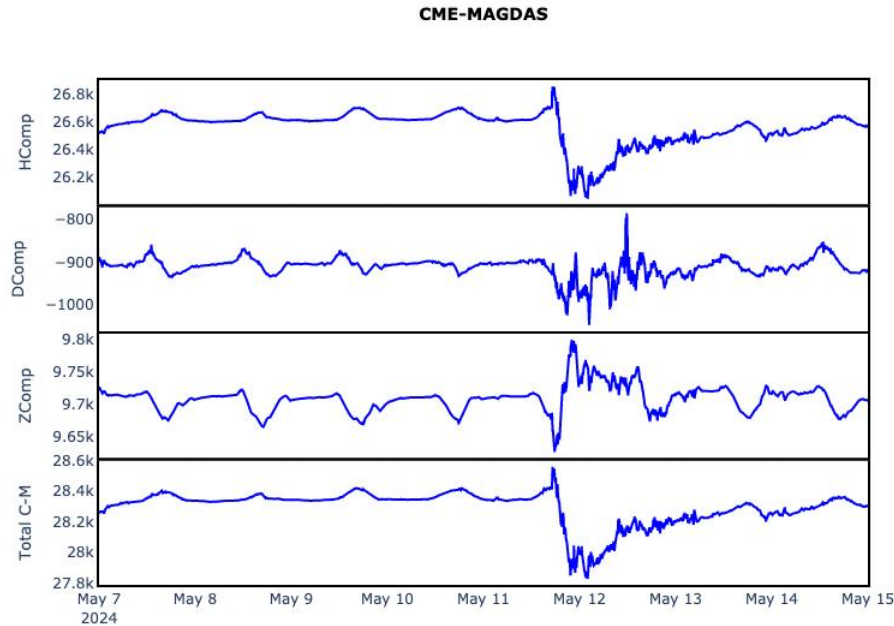


Figure 3. May, 2024 G5 storm, magnetic field components

equatorial ionization anomaly (EIA) during the storm, caused by disturbance electric fields and atmospheric winds, likely contributed to the TEC reduction, particularly in the crest regions (Batista et al., 2011).

Furthermore, the storm caused a significant reduction in the Earth’s magnetic field strength, commonly referred to as “Dst depression.” This decrease is primarily due to the enhanced ring current that forms during geomagnetic storms, as energetic particles from the solar wind are trapped in Earth’s magnetosphere and circulate in the ring current. The magnetic field generated by these particles opposes Earth’s own magnetic field, leading to the observed reduction, especially near the equator (Daglis et al., 1999).

Typically, as a geomagnetic storm progresses, initial disturbances in Earth’s magnetic field lead to sharp increases in ionization due to energetic particle precipitation. This can result in a short-term rise in TEC, followed by a gradual decline as the ionosphere returns to normal. The decay phase, during which TEC levels normalize, can take several hours to days, depending on the storm’s intensity and duration. In some cases, these disturbances can cause long-lasting fluctuations in TEC, referred to as “storm-time ionospheric anomalies” (Fuller-Rowell et al., 2008).

5 Conclusions

We examined the effect of geomagnetic storms on the variation of TEC (Total Electron Content) at the low-latitude station in Galapagos, which lies just below the equatorial anomaly region.

The geomagnetic storm on May 11, 2024, had a significant impact, decreasing TEC by approximately 30 TECU during the storm’s main phase. During this phase, “negative storm effects” commonly lead to a substantial depletion of ionospheric electron den-

sity, especially at low latitudes. This depletion reduces the ionospheric conductivity and weakens ionospheric currents, which in turn lowers the strength of the horizontal magnetic field. The reduction in ionospheric conductivity during a geomagnetic storm, particularly at low latitudes, causes a noticeable decline in ionospheric currents like the equatorial electrojet (EEJ). The weakening of the EEJ directly contributes to the observed decrease in the horizontal component of the magnetic field. In equatorial regions, such a drastic reduction in the horizontal magnetic field is a clear indicator of the weakened ionospheric current systems.

Our analysis demonstrates a strong correlation between the coronal mass ejection (CME) that triggered this storm and the geomagnetic indices Dst and Kp, with the Dst index reaching -400 nT. This value signals a major geomagnetic storm with potentially serious consequences for Earth's technological systems, underscoring the importance of continuous space weather monitoring to predict and mitigate such events. Monitoring CMEs, in particular, is crucial for forecasting geomagnetic disturbances.

Future research should aim to identify additional CME events and improve theoretical models describing magnetic field changes within CMEs. Moreover, real-time updates to ionospheric models, incorporating data from multiple sources, are essential for maintaining the accuracy of VTEC maps during geomagnetic storms. Advanced algorithms that can rapidly adjust to sudden changes in the ionosphere will be vital for enhancing space weather forecasting capabilities.

The May 11, 2024, geomagnetic storm serves as a reminder of the need for effective space weather monitoring and operational responses. While the storm had notable effects, they were largely mitigated due to preemptive monitoring and response efforts. This highlights the critical role of understanding and predicting space weather to safeguard technological infrastructure, including navigation and communication systems, from potential disruptions.

Data Availability

The Global Navigation Satellite System (GNSS) data used in this study is publicly available from the NASA Center for Earth Observing System Data and Information Services (CEOS DIS) archive. Users can access daily GNSS data at: <https://cdis.nasa.gov/archive/gnss/data/daily>.

The calculated Vertical Total Electron Content (VTEC) data used in this study is not publicly available. However, interested researchers can request access to the VTEC data by contacting the corresponding author ([ericsson.lopez@epn.edu.ec]).

As Applicable – Inclusion in Global Research Statement

Acknowledgments

References

- Aa, E., et al. (2024). Dynamic expansion and merging of the equatorial ionization anomaly during the 10–11 may 2024 super geomagnetic storm. *Remote Sensing*, 16(22), 4290. doi: 10.3390/rs16224290
- Abdu, M. A. (2005). Equatorial ionosphere–thermosphere system: Electrodynamics and irregularities. *Advances in Space Research*, 35(5), 771–787. doi: 10.1016/j.asr.2005.03.150
- Balan, N., et al. (2018). A brief review of equatorial ionization anomaly and ionospheric irregularities. *Earth and Planetary Physics*, 2(4), 257–275. doi: 10

- .26464/epp2018025
- Batista, I. S., et al. (2011). Equatorial ionization anomaly: The role of thermospheric winds and the effects of the geomagnetic field secular variation. In *Aeronomy of the earth's atmosphere and ionosphere* (pp. 317–328). Springer. doi: 10.1007/978-94-007-0326-1_23
- Chaithra, P., & Nagaraja, K. (2024). Ionospheric tec variations during an intense geomagnetic storm on 11 may 2024. *Research Square Preprint*. doi: 10.21203/rs.3.rs-4691095/v1
- Chen, P., et al. (2024). A new method for global ionospheric real-time modeling integrating ionospheric vtec short-term forecast results. *Journal of Geodesy*, *98*. doi: 10.1007/s00190-024-01911-9
- Ciraolo, L., et al. (2007). Calibration errors on experimental slant total electron content (tec) determined with gps. *Journal of Geodesy*, *81*(2), 111–120. doi: 10.1007/s00190-006-0093-1
- Daglis, I. A., et al. (1999). The terrestrial ring current: Origin, formation, and decay. *Reviews of Geophysics*, *37*(4), 407–438. doi: 10.1029/1999RG900009
- Fuller-Rowell, T. J., et al. (2008). Storm-time response of the thermosphere–ionosphere system. In *Aeronomy of the earth's atmosphere and ionosphere* (pp. 419–435). Springer. doi: 10.1007/978-94-007-0326-1_32
- GPS.gov. (2001). *2001 sps performance standard*. (Retrieved from <https://www.gps.gov/technical/ps/2001-SPS-performance-standard.pdf>)
- Hayakawa, H., et al. (2021). Temporal variations of the three geomagnetic field components at colaba observatory around the carrington storm in 1859. *arXiv preprint, arXiv:2109.13020*. doi: <https://arxiv.org/abs/2109.13020>
- Hernández-Pajares, M., Juan, J. M., Sanz, J., & Colombo, O. L. (2002). Improving the real-time ionospheric determination from gps sites at very long distances over the equator. *Journal of Geophysical Research: Space Physics*, *107*(A10), 1296. doi: 10.1029/2001JA009203
- Kamide, Y., et al. (1998). Current understanding of magnetic storms: Storm-substorm relationships. *Journal of Geophysical Research: Space Physics*, *103*(A8), 17705–17728. doi: 10.1029/98JA01426
- Kwak, Y.-S., et al. (2024). Observational overview of the may 2024 g5-level geomagnetic storm: From solar eruptions to terrestrial consequences. *Journal of Astronomy and Space Sciences*, *41*(3), 171–194. doi: 10.5140/JASS.2024.41.3.171
- Lanzerotti, L. J., et al. (2001). *Space weather effects on communications*. Springer. doi: 10.1007/978-94-010-0983-6_12
- Leitinger, R., Radicella, S. M., & Nava, B. (2008). Electron density models for assessment studies—new developments. *Space Weather*, *6*(9), S09001. doi: 10.1029/2008SW000411
- Li, H., Liu, X., & Wang, C. (2024). How solar wind controls the recovery phase morphology of intense magnetic storms. *Journal of Geophysical Research: Space Physics*, *129*(5), e2023JA032057. doi: 10.1029/2023JA032057
- Lin, J.-W. (2021). Geomagnetic storm related to disturbance storm time indices. *European Journal of Environment and Earth Sciences*, *2*(6), 199–204. doi: 10.24018/ejgeo.2021.2.6.199
- Luo, H., et al. (2023). Prediction of global ionospheric total electron content (tec) based on sam-convlstm model. *Space Weather*, *21*(12), e2023SW003707. doi: 10.1029/2023SW003707
- Matzka, J., et al. (2021). The geomagnetic kp index and derived indices of geomagnetic activity. *Space Weather*, *19*(5), e2020SW002641. doi: 10.1029/2020SW002641
- Misra, P., & Enge, P. (2006). *Global positioning system: Signals, measurements, and performance*. Ganga-Jamuna Press.
- Nagarajoo, K., & Fah, C. S. (2013, July). Significant of earth's magnetic field and

- ionospheric horizontal gradient to gps signals. In *2013 ieee international conference on space science and communication (iconspace)* (pp. 1–5). Melaka, Malaysia: IEEE. doi: 10.1109/IconSpace.2013.6599444
- Pirjola, R. (2002). Review on the calculation of surface electric and magnetic fields and geomagnetically induced currents in ground-based technological systems. *Surveys in Geophysics*, *23*(1), 71–90. doi: 10.1023/A:1014816009303
- Press, W. H., Teukolsky, S. A., Vetterling, W. T., & Flannery, B. P. (1992). *Numerical recipes in c: The art of scientific computing*. Cambridge University Press.
- Pulkkinen, A., et al. (2017). Geomagnetic storms and their impacts on the u.s. power grid. *Space Weather*, *15*(6), 713–725. doi: 10.1002/2016SW001501
- Ratovsky, K. G., et al. (2020). Statistical analysis of the ionospheric response to geomagnetic storms based on the data from global ionospheric maps. *Russian Journal of Physical Chemistry B*, *14*(5), 862–872. doi: 10.1134/S1990793120050243
- Shagimuratov, I. I., Klimenko, M. V., Efishov, I. I., Filatov, M. V., & Yakimova, G. A. (2024). Features of the november 7, 2022 geomagnetic storm development in the ionospheric total electron content observations. *Bulletin of the Russian Academy of Sciences: Physics*, *88*(3), 310–317. doi: 10.1134/S1062873823705457
- Shen, F., et al. (2022). Propagation characteristics of coronal mass ejections (cmes) in the corona and interplanetary space. *Reviews of Modern Plasma Physics*, *6*(8). doi: 10.1007/s41614-022-00069-1
- Simi, K. G., et al. (2013). Ionospheric response to a geomagnetic storm during november 8–10, 2004. *Earth, Planets and Space*, *65*(4), 343–350. doi: 10.5047/eps.2012.09.005
- Sun, X., et al. (2024). Statistical analysis of the correlation between geomagnetic storm intensity and solar wind parameters from 1996 to 2023. *Remote Sensing*, *16*(16), 2952. doi: 10.3390/rs16162952
- Tahir, A., et al. (2024). Multi-instrument observation of the ionospheric irregularities and disturbances during the 23–24 march 2023 geomagnetic storm. *Remote Sensing*, *16*(9), 1594. doi: 10.3390/rs16091594
- Yamazaki, Y., & Maute, A. (2017). Sq and eej—a review on the daily variation of the geomagnetic field caused by ionospheric dynamo currents. *Space Science Reviews*, *206*(1-4), 299–405. doi: 10.1007/s11214-016-0282-z